



00

SEMARAK ILMU
PUBLISHING
20210328161003318678-PI

CFD Letters

Journal homepage:

https://semarakilmu.com.my/journals/index.php/CFD_Letters/index

ISSN: 2180-1363



Comparison of Performance of Straight- and V-shaped Vanes Applied as Energy Saving Device to High-speed Boats

Ketut Suastika^{1,*}, Ahmad Septiawan Saputra¹, Adnan Faiz Fauzi¹, Ahmad Firdhaus²

¹ Department of Naval Architecture, Faculty of Marine Technology, Institut Teknologi Sepuluh Nopember, Surabaya, Indonesia

² Department of Naval Architecture, Universitas Diponegoro, Semarang, Indonesia

ARTICLE INFO

Article history:

Received 5 January 2023

Received in revised form 8 February 2023

Accepted 9 March 2023

Available online 1 October 2023

Keywords:

Energy-saving device; High-speed boat; Hull Vane[®]; Straight vane; V-shaped vane

ABSTRACT

Hull Vane[®] is a device, generally utilizing a straight vane, installed horizontally near the stern of a vessel below the water surface and oriented in the transverse direction of the vessel with the purpose to save fuel consumption and to increase the vessel's comfort. Because the bottom-hull form of a ship is generally curved, a non-straight vane may be more effective than a straight one when applied as Hull Vane[®]. The purpose of this study is to investigate the effectiveness of a V-shaped vane when applied as Hull Vane[®] on a 31 m high-speed crew boat. The study utilizes a computational fluid dynamics (CFD) method. CFD results show that the Hull Vane[®] decreased the bow-up trim of the boat, affected the boat's wetted surface area, and decreased the height of the waves generated by the boat. The wave-height reduction due to the V-shaped Hull Vane[®] is larger than the straight Hull Vane[®]. Further, the Hull Vane[®] significantly reduced the total resistance of the boat at Froude number $Fr = 0.34$ with a larger reduction resulted from the V-shaped Hull Vane[®] (25.09% reduction for the straight vane and 30.75% reduction for the V-shaped vane). The observed resistance reduction decreased with increasing speed, ascribed to a too-large vane's lift. The V-shaped Hull Vane[®] is more effective than the straight Hull Vane[®] in reducing the total resistance of the boat.

1. Introduction

Hull Vane[®] is a device, generally in the form of a straight vane, which is installed horizontally near the stern of a vessel below the water surface and oriented in the transvers direction of the vessel with the purpose to save fuel consumption and to increase the vessel's comfort. Hull Vane[®] was invented by van Oossanen in 1992 and it was patented in 2002. It can be retrofitted to an existing vessel or designed specifically for a newly constructed ship. The mechanism of the Hull Vane[®] leading to fuel saving and higher comfort level of a vessel, is described by Uithof *et al.*, [1]. An additional thrust can be generated by the Hull Vane[®] due to the angle between the water inflow and the vane chord line, which is affected by the stern form of the vessel. Further, it can reduce the height of the

* Corresponding author.

E-mail address: k_suastika@na.its.ac.id (Ketut Suastika)

waves generated by the vessel, thus decreasing the wave-making resistance, and it can reduce the vessel's motions in waves, resulting in a higher comfort level for crew and passengers.

Following the initial development of the Hull Vane® in 1990s, several studies reported its applications on different types of vessels, including yachts, patrol vessels, container ships, and ro-ro ferries and methods to improve its design process. A successful application of the Hull Vane® was reported by Uithof *et al.*, [1] when it was applied to a 55 m MV Karina fast supply vessel and a 42 m Alive superyacht. Bouckaert *et al.*, [2, 3] applied the Hull Vane® to a 108 m Holland-class OPV and reported a reduction in total fuel consumption up to 12.5%. Further, they reported that at the speed at which most fuel was consumed annually (17.5 knots) the total ship resistance was reduced by 15.3%. Other benefits include lower vertical acceleration at the helicopter deck, increased sailing range and increased top speed.

Uithof *et al.*, [4] compared the performances of a Hull Vane®, interceptors, trim wedges and ballasting in a study utilizing computational fluid dynamics (CFD) simulations. They reported that the Hull Vane® was the most efficient device in reducing ship resistance and in improving seakeeping performance. Further, they found a reduction in vessel's bow-up trim and sinkage. A resistance reduction was found at Fr between 0.2 and 0.8 reaching a maximum reduction up to 32.4% at $Fr = 0.35$. The position of the Hull Vane® in the longitudinal direction was found to have a significant effect on the ship resistance, while its position in the vertical direction played a minor role. They found that the best vane's position was that with vane's leading edge approximately 2.5 chord lengths behind the transom. At Fr between 0.6 and 0.8, the difference in the resulting ship resistance for the different vane's positions was rather small (less than 2%) as the flow behind the transom became more uniform with a resistance reduction between 10 and 12% in this Froude number range.

The feasibility and performance of a 500 GT trimaran yacht concept equipped with a Hull Vane® were reported by Uithof *et al.*, [5]. A comparison with an equivalent monohull vessel was made based on the criteria of lifetime costs, energy efficiency, luxury, and seakeeping comfort. They reported that the trimaran yacht with Hull Vane® performed better than the monohull equivalent in all four criteria referred to above. In another study, improvement of the nautical performance of a surface ship by using a Hull Vane® was reported by Ferre *et al.*, [6]. Celic *et al.*, [7] investigated the effect of the Hull Vane® on the ship resistance by using the open-source software OpenFOAM and reported a 22.9% reduction in the total resistance due to Hull Vane®. Further, Celic *et al.*, [8] developed a Machine-Learning (ML) based model that predicts the hull's total resistance in the presence of a Hull Vane® to avoid the time-consuming resistance evaluation of designs via a viscous flow solver.

Closely related to the present study, Suastika *et al.*, [9] and Riyadi and Suastika [10] reported the applications of a Hull Vane® on a 31 m high-speed crew boat (offshore supply vessel). In both studies, the authors chose NACA 64₁-212 section [11] for the Hull Vane® based on the largest lift to drag ratio among the sections considered in earlier studies [12, 13]. Suastika *et al.*, [9] and Riyadi and Suastika [10] found that the most optimum vane's position was that with the vane leading edge two chord lengths ($2c$) behind the ship transom, which is close to that reported by Uithof *et al.*, [4]. In addition, they recommended vane's submerged position of $3/4$ the boat's draft ($0.75 T$) below the water surface.

Studies on the Hull Vane® based on CFD simulations and model tests have been reported in earlier studies for different types of vessels. It was found that the Hull Vane® was only suitable for certain applications, not for all types of vessels, since in some applications a resistance increase was found. The buttock angle, the transom submergence and the stern form significantly determine the vane's performance as reported by Uithof *et al.*, [1]. It also depends on the vessel's speed (most favorable in Froude-number range $0.2 < Fr < 0.7$). As suggested by Uithof *et al.*, [1], bulk carriers and crude oil

carriers are not suitable for Hull Vane® applications. It is more suitable for applications on supply vessels, ferries, or patrol vessels (with length not shorter than 30 m due to investment costs).

To the best of our knowledge, a Hull Vane® always utilizes a straight vane in its applications. Other forms than a straight vane have not been explored in the existing literature of Hull Vane®, which is a gap in the Hull Vane® research and to be pursued in this study. Because the bottom-hull form of a ship is generally curved, a non-straight vane may be more effective than a straight vane. This leads to the introduction of a V-shaped vane in this study to be applied as Hull Vane®. The Hull Vane® is applied to a 31 m high-speed crew boat [9, 10], which has an aft bottom-hull form resembling a V-shape as shown in Figure 2. The study utilizes a computational fluid dynamics (CFD) method where the performance of the V-shaped Hull Vane® is compared with that of a straight Hull Vane®. The objective of the study is to investigate the effectiveness of the V-shaped Hull Vane® in reducing the total resistance of the boat, *i.e.*, to be used as an energy saving device (ESD). Seakeeping aspects and vessel comfort are not considered in this study.

2. Methodology

The boat considered in this study is the same as the boat reported by Suastika *et al.*, [9] and Riyadi and Suastika [10], *i.e.*, a 31 m high-speed crew boat. The boat’s main dimensions are summarized in Table 1. Figures 1a and b show, respectively, a straight vane and the V-shaped vane proposed in this study. As in the studies by Suastika *et al.*, [9] and Riyadi and Suastika [10], the span of the straight vane was set equal to the boat’s breadth, $s = B = 6.8$ m, and the chord length $c = 0.8$ m, resulting in vane’s aspect ratio $A = s/c = 8.5$. The angle of the V-shaped vane was set equal to the deadrise angle of the vessel, which is 8° as illustrated in Figure 2. To make the comparison between the straight- and V-shaped vanes fair, the wetted surface area (WSA) of both vanes was set approximately equal. (The WSA of the straight vane is 13.948 m² while the WSA of the V-shaped vane is 13.943 m², which differs only 0.0358%.)

Table 1
 Boat’s main dimensions

Parameter	Value
Length Overall LOA	31.20 m
Length between Perpendiculars LBP	28.80 m
Length at Waterline LWL	28.40 m
Breadth B	6.80 m
Depth H	2.75 m
Draft T	1.40 m
Displacement	104.68 t
Maximum speed	26 kn

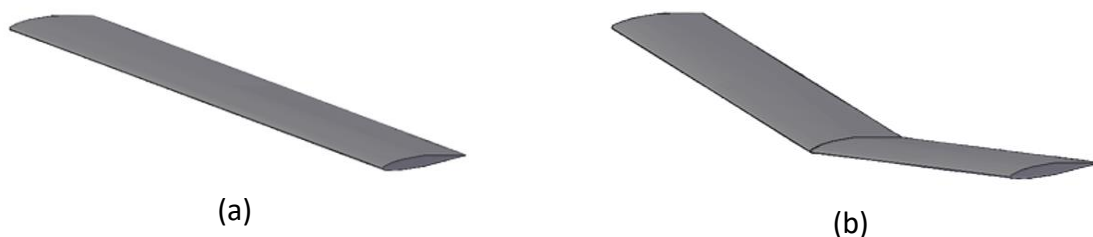


Fig. 1. The two vanes considered in this study: (a) Straight vane, usually used as a Hull Vane®; (b) The proposed V-shaped vane

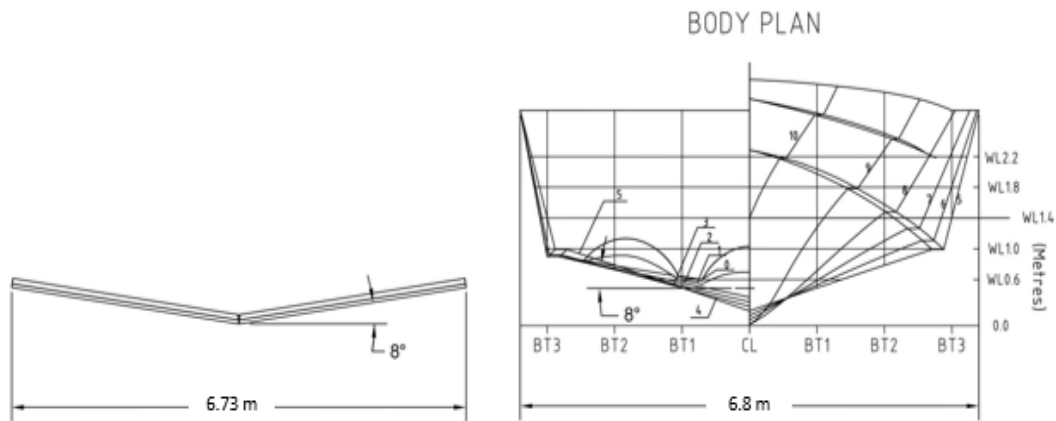


Fig. 2. Geometry of the V-shaped vane with an angle of 8° measured from the horizontal plane, which is equal to the deadrise angle of the boat shown in the right figure

Reynolds-averaged Navier-Stokes (RANS) simulations were conducted, utilizing Numeca FineTM/Marine [14-16], to study the performance of the straight- and V-shaped vanes as ESD. For incompressible flows, the RANS model consists of averaged continuity and momentum equations, which are given using tensor notation in a Cartesian coordinate system (x, y, z) in Eq. (1) and (2), respectively, as follows:

$$\frac{\partial U_i}{\partial x_i} = 0 \quad (1)$$

$$\frac{\partial U_i}{\partial t} + \frac{\partial(U_i U_j)}{\partial x_j} = -\frac{1}{\rho} \frac{\partial P}{\partial x_i} + \frac{\partial}{\partial x_j} \left[\nu \left(\frac{\partial U_i}{\partial x_j} + \frac{\partial U_j}{\partial x_i} \right) \right] - \frac{\partial \overline{u'_i u'_j}}{\partial x_j} \quad (2)$$

where t is time, U_i is the mean velocity component, P is the mean pressure, ν is the kinematic viscosity of the fluid, ρ is the fluid density, $-\rho \overline{u'_i u'_j}$ is the Reynolds stresses, and the indices $i, j = 1, 2, 3$ [17, 18]. A turbulence model is applied to calculate the Reynolds stresses $-\rho \overline{u'_i u'_j}$ in Eq. (2) for which the k - ω SST turbulence model [19] is chosen in this study. This turbulence model can predict the onset and amount of flow separation accurately [20].

2.1 Geometrical Models for the Boat and Vanes

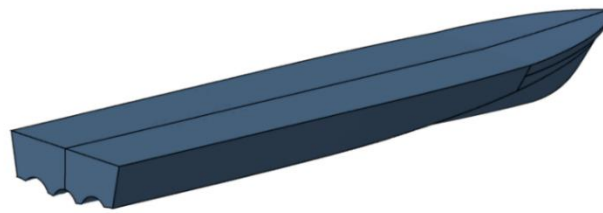
Three-dimensional (3-D) models for the boat without and with Hull Vane[®] were made with the aid of the Maxsurf Modeler software [21]. Following the results reported by Suastika *et al.*, [9, 13] and Riyadi and Suastika [10], the angle of attack of the Hull Vane[®], both the straight- and V-shaped Hull Vanes[®], was set 2° , measured counter-clockwise from the horizontal longitudinal axis (positive in the forward direction of the boat). These geometrical models are usually referred to as surface CAD models and are shown in Figure 3. (CAD stands for Computer Aided Design.) The surface CAD models are used as input in the following step of meshing in which the computational domain is defined and discretized into non-overlapping cells by using a finite volume method.

To ensure that the surface CAD model represents the prototype accurately, the hydrostatic characteristics of the CAD model were compared with those of the prototype. The results are tabulated in Table 2 for boat without Hull Vane[®]. Table 2 shows that the maximum percentage difference between the CAD model and the prototype is less than 2% for all parameters considered, indicating accurate geometrical modeling results.

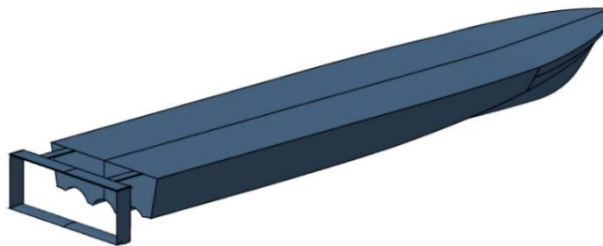
Table 2

Comparison of the hydrostatic characteristics between the CAD model and prototype for boat without Hull Vane®

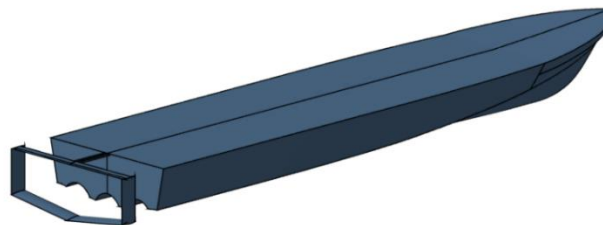
Parameter	Prototype	CFD model	Percentage difference [%]
Displacement [ton]	104.68	105.90	1.17
Wetted surface area WSA [m ²]	177.13	177.48	0.196
Block coefficient C_B	0.409	0.415	1.47
Midship coefficient C_M	0.470	0.479	1.89
Waterplane coefficient C_W	0.830	0.822	-0.964
Longitudinal center of buoyancy LCB measured from AP [m]	11.79	11.73	-0.483
Longitudinal center of floatation LCF measured from AP [m]	11.44	11.44	0.035



(a)



(b)



(c)

Fig. 3. Hull geometry of the crew boat: (a) Without Hull Vane®; (b) With straight Hull Vane®; (c) With V-shaped Hull Vane®

2.2 Meshing and Boundary Conditions

The turbulent flow with appropriate boundary conditions was solved by using a finite volume CFD method [17, 22, 23]. A multi-block structured grid was utilized to discretize the computational domain. Figure 4 shows the computational domain with the boat heading to the right. The domain boundaries are set as follows [22]. The inlet is located at $1.5 L$ upstream from the vessel and the outlet is located at $3.0 L$ behind the vessel, where L is the overall length of the boat (LOA). A side wall boundary is located at $1.5 L$ aside the symmetry-plane boundary. This is done because the computational domain is symmetric in the x - y plane. Therefore, only half of the computational

domain was modeled and simulated. The symmetry plane is the x - z plane as shown in Figure 4. Further, the bottom wall is located at $1.50 L$ below the vessel and the top wall is located at $1.0 L$ above the vessel.

The boundary conditions at the inlet, outlet and side wall are prescribed as far-field free stream velocity and pressure. At the bottom wall the pressure is prescribed as hydrostatic and at the top wall the boundary condition is prescribed as free slip. On the symmetry plane, symmetry boundary conditions are applied. The boundary condition on the ship hull is prescribed as no-slip, where a wall function is utilized. The heave and pitch motions of the boat are resolved in the simulations.

The interface between water and air (the free surface) needs special attention. The boat movement generates waves on the water surface. This generation of waves is modeled by using an interface capturing method for which a volume of fluid (VoF) method is utilized [24]. Two conditions must be satisfied on the free surface boundary, namely a kinematic boundary condition and a dynamic boundary condition. The kinematic boundary condition requires that the free surface be a sharp boundary separating the two fluids that allows no flow through it, while the dynamic boundary condition requires that the forces acting on the fluid at the free surface be in equilibrium [17]. Neglecting the surface tension, the dynamic boundary condition simplifies to that the pressure on the free surface is equal to the local atmospheric pressure.

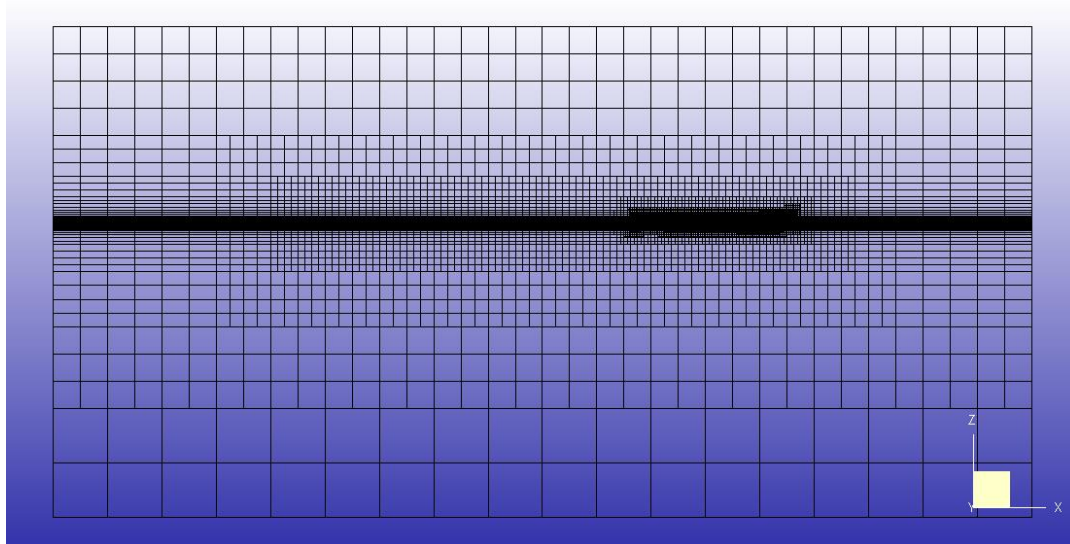


Fig. 4. Side view of the discretized computational domain utilizing a multi-block structured grid, showing the boat heading to the right, with computational boundaries

2.3 Grid Independence Tests

Grid independence tests were conducted by considering first the case of boat without Hull Vane[®]. Based on these results, a standard procedure was then followed to obtain an optimum mesh for the case of boat with Hull Vane[®]. In the grid independence tests, the percentage difference between two subsequent simulation results of total resistance was calculated, in which the number of cells in the latter simulation was approximately twice that in the former. The results for boat's speed $V = 11$ knots ($Fr = 0.34$) are summarized in Table 3, showing four runs with increasing number of cells used in the simulation for the case of boat without Hull Vane[®].

Table 3 shows that both the total resistance R_T and the magnitude of the percentage difference $e_{n+1, n}$ decrease monotonically with increasing number of cells. It is expected that for a very large number of cells (in the limit N tends to infinity) R_T will converge to an asymptotic value, which is in

this case approximately 24.79 kN. A percentage difference of less than 2% is used as a criterion for the grid independence tests [25]. The magnitude of the percentage difference between run number 4 with $N = 4,701,551$ and run number 3 with $N = 2,294,875$ is 1.35%. Based on the above results, the number of cells $N = 2,294,875$ was chosen as an optimum number of cells for the simulations of boat without Hull Vane®.

Table 3

Total ship resistance R_T calculated using an increasing number of cells in the simulation for the case of boat without Hull Vane® at the speed $V = 11$ knots ($Fr = 0.34$)

Run number n	Number of cells N	Total resistance R_T [kN]	Percentage difference $e_{n+1, n}$ [%]
1	637,183	27.76	-
2	1,223,562	25.76	-7.76
3	2,294,875	25.12	-2.56
4	4,701,551	24.79	-1.35

For the case of boat with Hull Vane®, either straight Hull Vane® or V-shaped Hull Vane®, further discretization of the computational domain (with $N = 2,294,875$) was carried out by using the default setting of Numeca FINE™/Marine [14-16]. This further discretization of computational domain resulted in number of cells which is larger than 2,294,875, *i.e.*, $N = 2,829,861$ for the case with straight Hull Vane® and $N = 2,499,050$ for the case with V-shaped Hull Vane®. For the reason of saving computational time, grid independence tests were not carried out for all boat's speeds. The results for the speed $V = 11$ knots are considered representative for all the other speeds.

2.4 Verification of the CFD Calculation Results

To get confidence with the CFD results, the results for the case of boat without Hull Vane® are compared with the results obtained from Savitsky's empirical method [26] and with the experimental data of Riyadi and Suastika [10]. The comparisons are summarized in Table 4 for boat's speeds $V = 17, 20, 23$ and 26 knots. The subscripts Sav, exp and CFD in Table 4 refer to, respectively, Savitsky's method, experimental data and CFD results. Table 4 shows that the results from Savitsky's method are closer than the experimental data to the CFD results. The maximum magnitude of percentage difference between the results of Savitsky's method and CFD is 3.42%, while the maximum magnitude of percentage difference between the experimental data and CFD results is 5.32%. A percentage difference of approximately 5% between experimental data and CFD results is rather common in practice. Further, Table 4 shows that the CFD results are close to the results from Savitsky's method and the experimental data of Riyadi and Suastika [10] with a maximum percent error of approximately 5%. This observation gives confidence in the CFD method to be utilized in the study of straight- and V-shaped Hull Vanes®. The results are presented in the following section.

Table 4

Total ship resistance R_T for the case of boat without Hull Vane® obtained from CFD simulations, Savitsky's method [26] and experiments [10]

V [knots]	Fr	CFD [kN]	Savitsky's method [25] [kN]	Experimental data [9] [kN]	$e_{Sav, CFD}$ [%]	$e_{exp, CFD}$ [%]
17	0.52	59.04	57.02	-	-3.42	-
20	0.62	72.33	71.31	72.11	-1.41	-0.300
23	0.71	82.54	82.93	-	0.463	-
26	0.80	92.25	89.61	97.16	-2.87	5.32

3. Results and Discussion

In this section, the CFD results of boat with V-shaped Hull Vane[®] are compared with the results of boat with straight Hull Vane[®]. Further, the results with Hull Vane[®] are compared with the results of the reference case of boat without Hull Vane[®]. Table 5 summarizes the total resistance R_T of the boat for the three cases considered, namely, (i) without Hull Vane[®], (ii) with straight Hull Vane[®] and (iii) with V-shaped Hull Vane[®]. The subscripts No, Str and Vsh in Table 5 refer to, respectively, without Hull Vane[®], with straight Hull Vane[®] and with V-shaped Hull Vane[®].

Table 5 shows that, at the speed $V = 11$ knots ($Fr = 0.34$), both the straight- and V-shaped Hull Vanes[®] resulted in a significant decrease of total resistance, with a resistance reduction of 25.09% for the boat with straight Hull Vane[®] and 30.75% for the boat with V-shaped Hull Vane[®]. This observation is encouraging in view of the purpose of the Hull Vane[®] as ESD. Further, at the speed $V = 17$ knots ($Fr = 0.52$) the straight Hull Vane[®] resulted in a 7.31% increase of total resistance, while the V-shaped Hull Vane[®] resulted in a 2.34% decrease of total resistance. At larger speeds ($V = 20$ and 26 knots; $Fr = 0.62$ and 0.80), both Hull Vanes[®] resulted in an increase of total resistance. The increase in total resistance due to the straight Hull Vane[®] is larger than that due to the V-shaped Hull Vane[®]. At the maximum speed ($Fr = 0.80$), the resistance increase is maximum, with a value of 31.99% for the straight Hull Vane[®] and 16.84% for the V-shaped Hull Vane[®].

Table 5

Comparison of total ship resistance R_T for the cases without Hull Vane[®], with straight Hull Vane[®] and with V-shaped Hull Vane[®]

V [knots]	Fr	Without Hull Vane [®] [kN]	Straight Hull Vane [®] [kN]	V-shaped Hull Vane [®] [kN]	$e_{Str, No}$ [%]	$e_{Vsh, No}$ [%]
11	0.34	25.12	18.82	17.40	-25.09	-30.75
17	0.52	59.04	63.36	57.66	7.31	-2.34
20	0.62	72.33	83.35	74.47	15.24	2.97
26	0.80	92.25	121.76	107.79	31.99	16.84

The above results show that the Hull Vane[®] most effectively works at the Froude number $Fr = 0.34$. Uithof *et al.*, [4] reported a maximum reduction of ship resistance of 32.4% at $Fr = 0.35$ when a Hull Vane[®] was applied. In this regard, the result of this study is in a good agreement with the result reported by Uithof *et al.*, [4]. However, Uithof *et al.*, [4] found a resistance reduction in the Froude number range between 0.2 and 0.8, while the present study only shows a resistance reduction at $Fr = 0.34$ for the boat with straight Hull Vane[®] and at Fr between 0.34 and 0.52 for the boat with V-shaped Hull Vane[®]. This indicates that the Hull Vanes[®] proposed in this study still need improvements. Further, a comparison between the results of the straight- and V-shaped Hull Vanes[®] shows that the V-shaped Hull Vane[®] is more effective than the straight Hull Vane[®] in reducing the total resistance of the boat.

To gain more insight into the above observations, the running trim and WSA of the boat were calculated at the speeds $V = 11, 17, 20$ and 26 knots. A positive running trim corresponds to a bow-up trim, while a negative running trim corresponds to a bow-down trim. Results of calculations of the running trim and WSA are summarized in Table 6. The calculation of WSA for the cases of boat with Hull Vane[®] also includes the WSA of the vane itself, which is approximately 14 m^2 . In addition to the running trim and WSA, the wave patterns generated by the boat are visualized and are shown in Figures 5 and 6 for boat's speeds $V = 11$ and 26 knots, respectively (the smallest and largest speed considered in the study).

Table 6 shows that at the speed $V = 11$ knots ($Fr = 0.34$), the boat underwent a bow-down trim in all the cases. The smallest bow-down trim is observed for the boat without Hull Vane[®] with a value of -0.4266° . The Hull Vane[®] resulted in a larger bow-down trim because of the lift force generated by the vane, giving a bow-down couple about the boat's center of floatation. The boat with straight Hull Vane[®] has a slightly larger trim (-1.095°) than that with V-shaped Hull Vane[®] (-1.081°). Further, the Hull Vanes[®] reduced the WSA of the boat as compared to the reference case of boat without Hull Vane[®]. The boat with V-shaped Hull Vane[®] has the smallest WSA with a value of 180.66 m^2 .

Considering the waves generated by the boat, Figure 5 shows that at the speed $V = 11$ knots ($Fr = 0.34$) the Hull Vane[®] reduced the height of the waves generated by the boat, where the V-shaped Hull Vane[®] resulted in the smallest wave height. Earlier studies, *e.g.*, Uithof *et al.*, [1, 4], Suastika *et al.*, [9] and Riyadi and Suastika [10] also reported a reduction in wave height due to Hull Vane[®]. A smaller wave height indicates a smaller wave-making resistance, so the V-shaped Hull Vane[®] resulted in the smallest boat's wave-making resistance. Figure 5 also shows that the wave pattern consists of transverse waves propagated in the direction of the ship course and divergent waves propagated in the direction making an angle with the ship course. The combined effects of running trim, WSA and height of the waves generated by the boat resulted in the smallest total resistance for the boat with V-shaped Hull Vane[®] at this speed (see Table 5).

Table 6

Running trim and wetted surface area (WSA) of the boat for the cases without Hull Vane[®], with straight Hull Vane[®] and with V-shaped Hull Vane[®]

V [knots]	Fr	Case	Running trim [deg]	WSA [m ²]
11	0.34	Without Hull Vane [®]	-0.4266	182.90
		Straight Hull Vane [®]	-1.095	182.00
		V-shaped Hull Vane [®]	-1.081	180.66
17	0.52	Without Hull Vane [®]	+0.8587	188.26
		Straight Hull Vane [®]	-0.6658	201.13
		V-shaped Hull Vane [®]	-0.5789	195.57
20	0.62	Without Hull Vane [®]	+1.377	188.99
		Straight Hull Vane [®]	-0.2565	202.45
		V-shaped Hull Vane [®]	-0.1961	195.63
26	0.80	Without Hull Vane [®]	+1.534	192.34
		Straight Hull Vane [®]	-0.5049	199.06
		V-shaped Hull Vane [®]	-0.3999	190.95

At larger speeds ($V = 17$ and 20 knots; $Fr = 0.52$ and 0.62), the bow-down trim decreased due to planing of the hull. Hull planing results in a bow-up trim. At these speeds, the boat without Hull Vane[®] underwent a bow-up trim ($+0.8587^\circ$ and $+1.377^\circ$ at the speeds 17 and 20 knots, respectively) while the boat with Hull Vane[®] underwent a bow-down trim. The boat with V-shaped Hull Vane[®] has the smallest trim (-0.5789° and -0.1961° at the speeds 17 and 20 knots, respectively). The Hull Vane[®] increased the WSA at these speeds with the largest WSA observed for the boat with straight Hull Vane[®] (201.13 m^2 and 202.45 m^2 at the speeds 17 and 20 knots, respectively). The increase in WSA and the bow-down trim resulted in a rather poor performance of the Hull Vane[®] (see Table 5).

At the maximum speed, $V = 26$ knots ($Fr = 0.80$), the lift force generated by the vanes became largest with corresponding bow-down couple about the boat's center of floatation. However, the resulting bow-down trim is compensated by the bow-up trim due to hull planing. Table 6 shows that the boat without Hull Vane[®] underwent a rather large bow-up trim ($+1.534^\circ$) due to hull planing. Further, the boat with straight Hull Vane[®] underwent the largest bow-down trim (-0.5049°) and it had also the largest WSA (199.06 m^2). This explains that the boat with straight Hull Vane[®] has the

largest resistance among the three cases considered at the maximum speed (see Table 5). The boat with V-shaped Hull Vane[®] also underwent a bow-down trim, but with a smaller value than the boat with straight Hull Vane[®] (-0.3999°). An important observation is that the boat with Hull Vane[®], either straight- or V-shaped Hull Vane[®], underwent a bow-down trim at all speeds. This indicates a too-large vane's lift. Reducing the vane's lift is recommended to improve the Hull Vane[®] performance.

Considering the waves generated by the boat, at the speed $V = 26$ knots ($Fr = 0.80$) the boat generated higher waves than at the speed $V = 11$ knots ($Fr = 0.34$), as expected (compare Figure 6 with Figure 5). Further, Figure 6 shows that the Hull Vane[®] reduced the height of the waves generated by the boat, with the smallest wave height resulted from the boat with V-shaped Hull Vane[®]. This observation is consistent with the observation made at the speed $V = 11$ knots. However, a further comparison between Figures 5 and 6 shows that at the speed $V = 26$ knots the wave pattern is dominated by the divergent waves. This observation is consistent with the theoretical prediction given by Faltinsen [27].

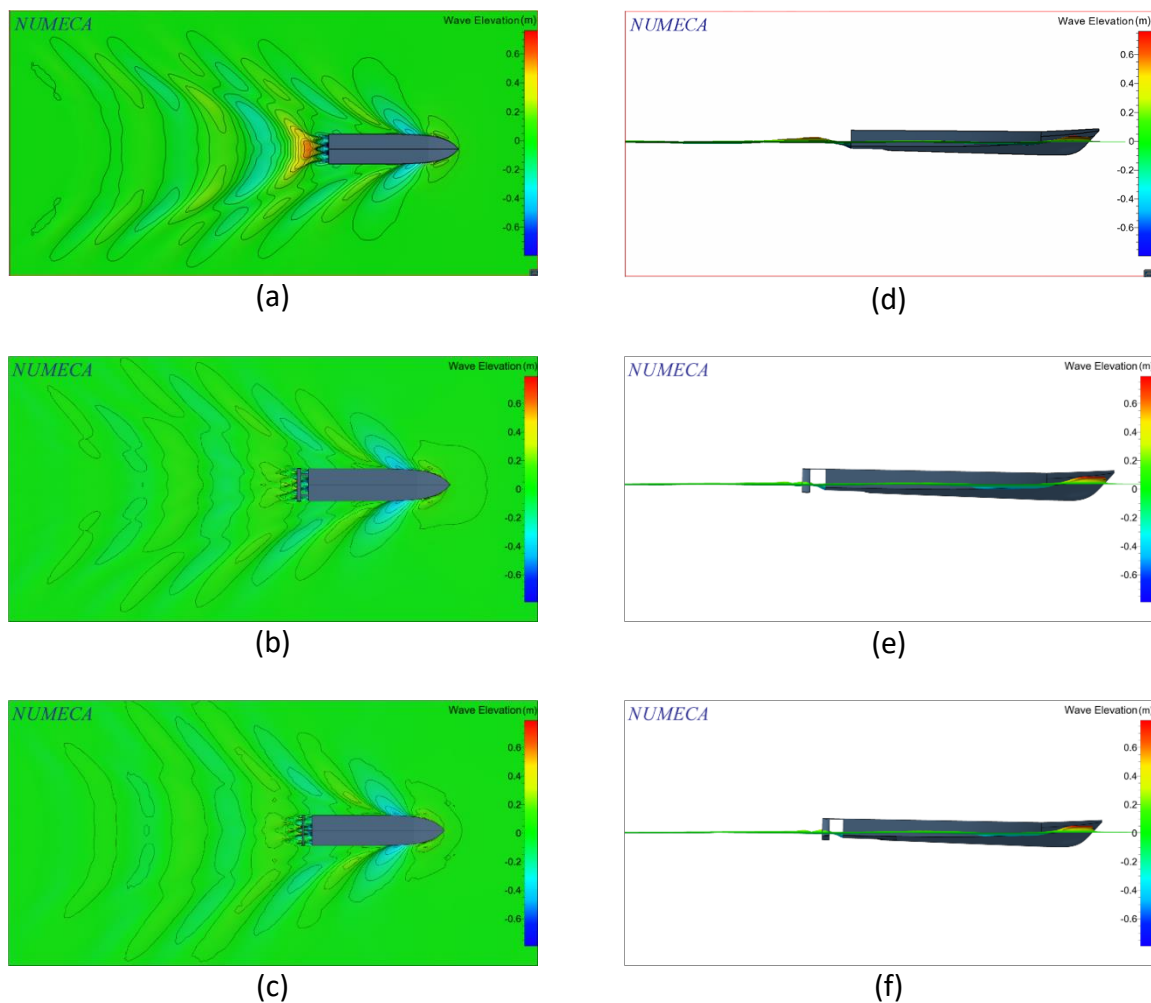


Fig. 5. Wave patterns at speed $V = 11$ knots ($Fr = 0.34$). The left column (a, b, c) shows above views while the right column (d, e, f) shows side views; (a, d) Without Hull Vane[®]; (b, e) With straight Hull Vane[®]; (c, f) With V-shaped Hull Vane[®]

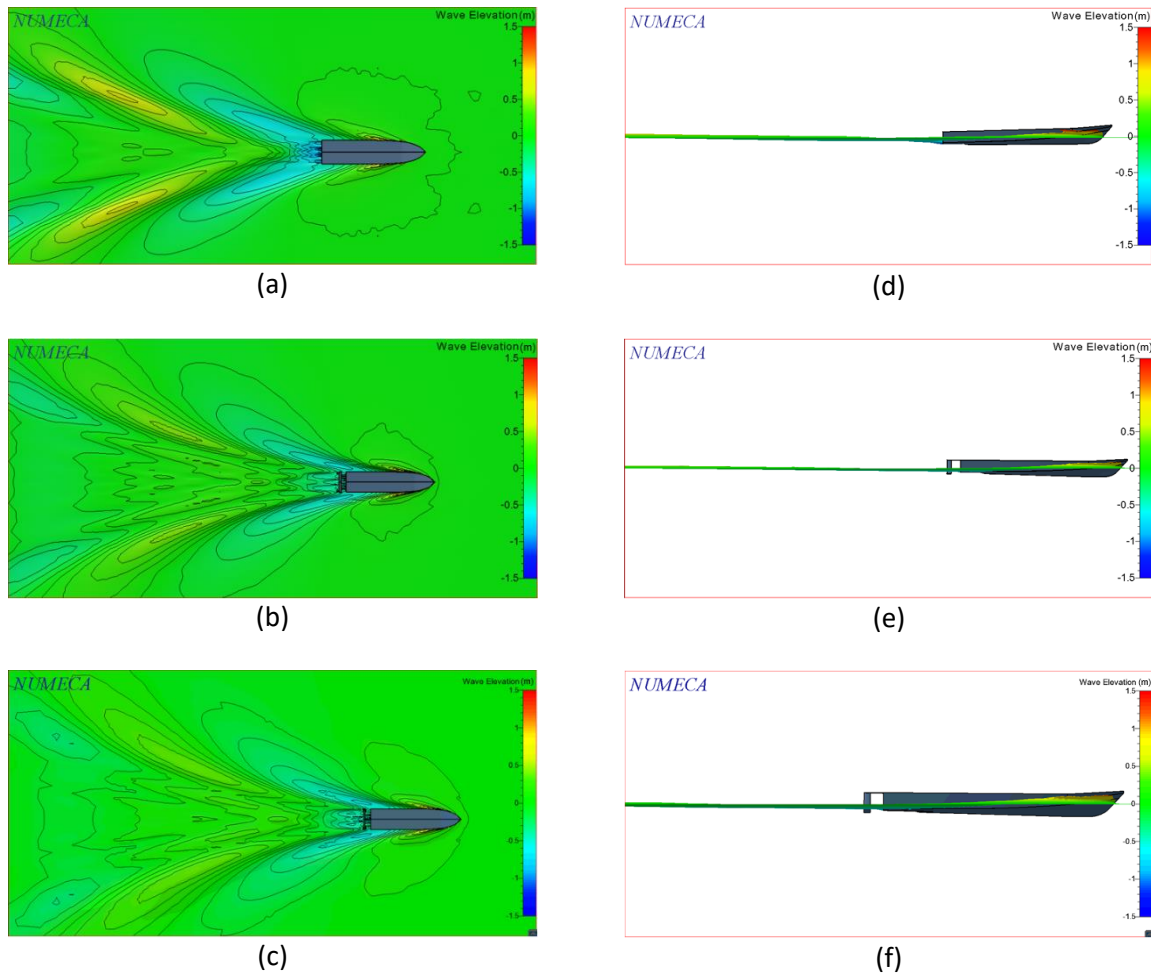


Fig. 6. Wave patterns at speed $V = 26$ knots ($Fr = 0.80$). The left column (a, b, c) shows above views while the right column (d, e, f) shows side views; (a, d) Without Hull Vane[®]; (b, e) With straight Hull Vane[®]; (c, f) With V-shaped Hull Vane[®]

4. Conclusions

A V-shaped vane is proposed as Hull Vane[®] in this study. This application is novel because Hull Vane[®] usually utilizes a straight vane. The Hull Vane[®] was applied to a 31 m high-speed crew boat in a study utilizing a CFD method. The performance of the V-shaped Hull Vane[®] is compared with that of a straight Hull Vane[®]. CFD results show that the Hull Vane[®], either straight- or V-shaped Hull Vane[®], decreased the bow-up trim of the boat, affected the boat's WSA, and decreased the height of the waves generated by the boat. The boat with V-shaped Hull Vane[®] generated the lowest wave height, thus smallest wave-making resistance. The Hull Vane[®] significantly reduced the total resistance of the boat at $Fr = 0.34$ with 30.75% reduction for the V-shaped Hull Vane[®] and 25.09% reduction for the straight Hull Vane[®]. However, the resistance reduction decreased with increasing speed (Froude number), ascribed to a too-large vane's lift. Although improvement of the Hull Vane[®] design is required, it can be concluded that the V-shaped Hull Vane[®] is more effective than the straight Hull Vane[®] in reducing the total resistance of the boat.

Acknowledgement

The authors gratefully acknowledge the financial support for this work from Institut Teknologi Sepuluh Nopember (ITS), Surabaya, Indonesia, under the project scheme Publication Writing and IPR Incentive Program (PPHKI) 2022.

References

- [1] Uithof, Kasper, P. Van Oossanen, N. Moerke, P. G. Van Oossanen, and K. S. Zaaijer. "An update on the development of the Hull Vane." In *9th International Conference on High-Performance Marine Vehicles (HIPER), Athens*, pp. 211-221. 2014.
- [2] Bouckaert, B., K. Uithof, P. G. Van Oossanen, and N. Moerke. "Hull vane on Holland-Class OPVs—A CFD analysis of the effects on seakeeping." In *13th International Naval Engineering Conference and Exhibition (INEC), Bristol*. 2016.
- [3] Bouckaert, Bruno, Kasper Uithof, Perry van Oossanen, Niels Moerke, Bart Nienhuis, and Jan van Bergen. "A life-cycle cost analysis of the application of a Hull Vane to an Offshore Patrol Vessel." In *SNAME International Conference on Fast Sea Transportation*, p. D021S006R001. SNAME, 2015. <https://doi.org/10.5957/FAST-2015-028>
- [4] Uithof, Kasper, N. Hagemester, B. Bouckaert, P. G. Van Oossanen, and N. Moerke. "A systematic comparison of the influence of the Hull Vane®, interceptors, trim wedges, and ballasting on the performance of the 50m AMECRC series# 13 patrol vessel." *Proc. Warship* (2016).
- [5] Uithof, K., P. G. van Oossanen, and F. Bergsma. "The feasibility and performance of a trimaran yacht concept equipped with a Hull Vane®." *Design and Construction of Super and Mega Yachts* (2015). <https://doi.org/10.3940/rina.msy.2015.16>
- [6] Ferreé, H., Philippe Goubault, Camille Yvin, and Bruno Bouckaert. "Improving the nautical performance of a surface ship with the Hull Vane® appendage." *Association Technique Maritime et Aéronautique. Numéro 2738* (2019).
- [7] Celik, C., D. B. Danisman, P. Kaklis, and S. Khan. "An investigation into the effect of the Hull Vane on the ship resistance in OpenFOAM." *Sustainable Development and Innovations in Marine Technologies* (2019): 136-141. <https://doi.org/10.1201/9780367810085-17>
- [8] Çelik, Cihad, Devrim Bülent Danışman, Shahroz Khan, and Panagiotis Kaklis. "A reduced order data-driven method for resistance prediction and shape optimization of hull vane." *Ocean Engineering* 235 (2021): 109406. <https://doi.org/10.1016/j.oceaneng.2021.109406>
- [9] Suastika, K., A. Firdhaus, R. Akbar, W. D. Aryawan, and I. K. A. P. Utama. "Experimental and numerical study of ship resistance due to variation of hull vane® positioning in the longitudinal direction," in *Proceedings of International Conference on Ship and Offshore Technology*, 2019, pp. 5–14.
- [10] Riyadi, Soengeng, and Ketut Suastika. "Experimental and Numerical Study of High Froude-number Resistance of Ship Utilizing a Hull Vane®: A Case Study of a Hard-chine Crew Boat." *CFD Letters* 12, no. 2 (2020): 95-105.
- [11] Abbott, Ira H., and Albert E. Von Doenhoff. *Theory of wing sections: including a summary of airfoil data*. Courier Corporation, 2012.
- [12] Suastika, K., and Apriansyah. "Effects of stern-foil submerged elevation on the lift and drag of a hydrofoil craft." In *IOP Conference Series: Earth and Environmental Science*, vol. 135, no. 1, p. 012003. IOP Publishing, 2018. <https://doi.org/10.1088/1755-1315/135/1/012003>
- [13] Suastika, Ketut, Affan Hidayat, and Soengeng Riyadi. "Effects of the application of a stern foil on ship resistance: A case study of an Orela crew boat." *International Journal of Technology* 8, no. 7 (2017): 1266-1275. <https://doi.org/10.14716/ijtech.v8i7.691>
- [14] Numeca International. "FINE™/Marine 7.2 Theory Guide," Belgium, 2018.
- [15] Suastika, I. K., A. F. Fauzi, A. S. Saputra, I. K.A.P. Utama, A. Firdhaus, Sutardi, and M. Hariadi. "Benchmark tests of FINE™/Marine CFD code for the calculation of ship resistance at high Froude numbers," in *Proceedings of International Conference Royal Institution of Naval Architects*, 2021. <https://doi.org/10.3940/rina.icsotindonesia.2021.14>
- [16] FINE™/Marine. "User Manual: Flow Integrated Environment for Marine Hydrodynamics," 2021. [Online]. Available: <https://www.numeca.com/product/fine-marine>
- [17] Ferziger, J. H. and M. Perić. *Computational Methods for Fluid Dynamics*. 2002. <https://doi.org/10.1007/978-3-642-56026-2>
- [18] Cebeci, T., J. P. Shao, F. Kafyeke, and E. Laurendau. *Computational Fluid Dynamics for Engineers*. 2005.
- [19] Menter, F. R. "Two-equation eddy-viscosity turbulence models for engineering applications," *AIAA Journal*, vol. 32, no. 8, 1994. <https://doi.org/10.2514/3.12149>
- [20] Bardina, Jorge E., Peter G. Huang, and Thomas J. Coakley. *Turbulence modeling validation, testing, and development*. No. A-976276. 1997. <https://doi.org/10.2514/6.1997-2121>
- [21] Maxsurf. "MAXSURF Naval Architecture Software," <https://maxsurf.net/>, Jun. 25, 2021.
- [22] Versteeg, Henk Kaarle, and Weeratunge Malalasekera. *An introduction to computational fluid dynamics: the finite volume method*. Pearson education, 2007.
- [23] Darwish, Marwan, and Fadl Moukalled. *The finite volume method in computational fluid dynamics: an advanced introduction with OpenFOAM® and Matlab®*. Springer, 2016.

- [24] Nichols, B. D., C. W. Hirt, and R. S. Hotchkiss. "Volume of fluid (VOF) method for the dynamics of free boundaries." *J. Comput. Phys* 39 (1981): 201-225. [https://doi.org/10.1016/0021-9991\(81\)90145-5](https://doi.org/10.1016/0021-9991(81)90145-5)
- [25] Anderson Jr, J. D. *Computational Fluid Dynamics: The Basics with Applications*, New York: McGraw-Hill, Inc., 1995.
- [26] Savitsky, Daniel. "Hydrodynamic design of planing hulls." *Marine Technology and SNAME News* 1, no. 04 (1964): 71-95. <https://doi.org/10.5957/mt1.1964.1.4.71>
- [27] Faltinsen, Odd M. *Hydrodynamics of high-speed marine vehicles*. Cambridge university press, 2005. <https://doi.org/10.1017/CBO9780511546068>